# Cloud-Top Heights from *GOES-8* and *GOES-9* Stereoscopic Imagery

DONALD P. WYLIE AND DAVID SANTEK

*Space Science and Engineering Center, University of Wisconsin—Madison, Madison, Wisconsin*

DAVID O'C. STARR

*NASA/Goddard Space Flight Center, Greenbelt, Maryland*

(Manuscript received 14 April 1997, in final form 12 September 1997)

ABSTRACT

Operational satellite data from *GOES-8* and *GOES-9* were used to make stereoscopic measurements of cloud heights during the National Aeronautics and Space Administration's Subsonic Aircraft: Contrail and Cloud Effects Special Study program. The stereoscopic data were used to differentiate between boundary layer wave clouds and cirrus in the mid- and upper troposphere. This separation was difficult to evaluate from radiometric data alone. Stereographic cloud height analysis provided a definitive result. The technique used for calculating cloud heights is described. *GOES-8* and *-9* data were better suited for stereoscopic measurements than data from previous satellites.

## 1. Introduction

The use of two geostationary meteorological satellites for stereoscopic measurements of cloud-top heights was pioneered by Hasler (1981) and Hasler et al. (1983) using the original Geostationary Operational Environmental Satellites (GOES). This tool showed promise for monitoring cumulonimbus clouds (Rodgers et al. 1983; Hasler et al. 1991), for research on convective clouds (Fujita 1982; Mack et al. 1983), and for developing climatological cloud monitoring systems (Wylie et al. 1989). Unfortunately, the capability to acquire stereoscopic data from the operational geostationary satellites was lost with the failure of *GOES-6* in the late 1980s. The potential for stereoscopic data returned with the next generation of geostationary satellites, *GOES-8* and *GOES-9* (see Menzel and Purdom 1994) but, to the authors' knowledge, has not been significantly used.

The heights of cloud tops are often difficult to determine from satellite data. The easiest method is to use the blackbody temperature derived from the upwelling radiance measured in the 11-$\mu$m window channel and compare this temperature to a sounding to find the height. This method works for simple clouds that are large enough to cover the satellite's field of view (FOV) and dense enough so that all the measured radiation comes from the cloud top or an altitude close to it. It fails for clouds smaller than the satellite sensor FOV (Wielicki and Parker 1992) and for clouds that transmit terrestrial radiation (Rossow 1989). In these cases, the observed blackbody radiative temperature will be warmer than the true temperature of the cloud tops. Wylie et al. (1994) reported that 40% of the global National Oceanic and Atmospheric Administration (NOAA) High-Resolution Infrared Sounder (HIRS) data contained clouds with top heights colder than their blackbody radiative temperatures that necessitated more elaborate methods for estimating cloud-top altitudes.

Several correction methods have been developed for cloud size and infrared transmission effects. Visible reflectance measurements have been used to estimate the infrared transmission (Rossow 1989; Rossow and Gardner 1993; Minnis et al. 1993a; Minnis et al. 1993b). The partially absorbing $CO_2$ channels in the infrared between 13 and 15 $\mu$m have also been used (Wylie and Menzel 1989; Wylie et al. 1994; Menzel et al. 1992; Susskind et al. 1987). Global climatologies of cloud-top heights are being compiled using such techniques, for example, the International Satellite Cloud Climatology Project (ISCCP; see Rossow and Schiffer 1991) and the Wisconsin HIRS Cloud Climatology (Wylie et al. 1994).

Although stereoscopic data cannot be obtained globally from the GOES satellites, they still are important tools that can be used to enhance the understanding and interpretation of other cloud datasets. Wylie and Menzel (1989) used data from the previous GOES system to verify cloud heights estimated from 13–15-$\mu$m infrared satellite data. Recently, a distinctive wave pattern in

*Corresponding author address:* Donald P. Wylie, Space Science and Engineering Center, University of Wisconsin—Madison, 1225 West Dayton Street, Madison, WI 53706.
E-mail: donw@ssec.wisc.edu

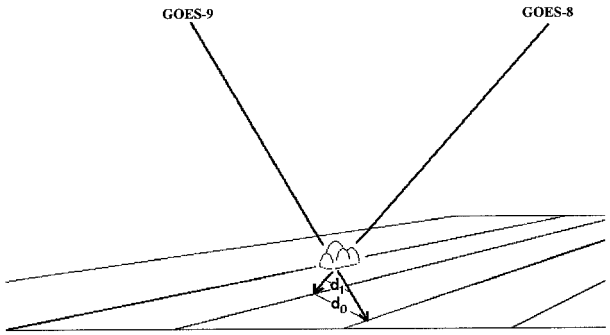


FIG. 1. A schematic of the pointing vectors to a cloud object from the two satellites. Here, $d_0$ and $d_1$ are the parallax displacement distances between the apparent positions of the cloud in the images from the two satellites. Further, $d_0$ refers to an assumption of the objects being on the earth's surface, while $d_1$ assumes the object is 1 km above the surface.

cloud fields observed in Oklahoma on 21 April 1996 during the National Aeronautics and Space Administration's (NASA) Subsonic Aircraft: Contrail and Cloud Effects Special Study (SUCCESS) presented a difficult situation for the other cloud height measuring techniques. Stereoscopic data from *GOES-8* and *GOES-9* were sought to determine whether the cloud waves, which were obvious on GOES imagery, corresponded to wave patterns detected in mid- and upper tropospheric cirrus by other SUCCESS sensors or were associated with boundary layer clouds below the cirrus. To answer this question, a technique used by Wylie and Menzel (1989) on *GOES-6* and *GOES-7* data was applied to the newer GOES data. This technique is a refinement of Hasler (1981) that was not previously documented. Because of the new availability of stereoscopic data, we report on our use of it and discuss how stereoscopic data can be used in the future with the new GOES satellites.

## 2. The stereoscopic technique

Cloud height measurements from stereoscopic satellite data are very artfully described in Hasler (1981) and Hasler et al. (1991). The height measurement uses the parallax shift in cloud locations caused by the slanted views of the satellites. In every slanted view, the apparent cloud location is shifted away from the cloud's nadir location because the cloud is above the earth, while the registration system is forced to assume that it is on the earth's surface. The registration system solves for the intersection of the pointing vector of the satellite sensor with the earth's surface. Since the cloud is above the surface and its height is not yet known, the cloud's location is displaced—the parallax shift. The magnitude of the parallax shift is proportional to

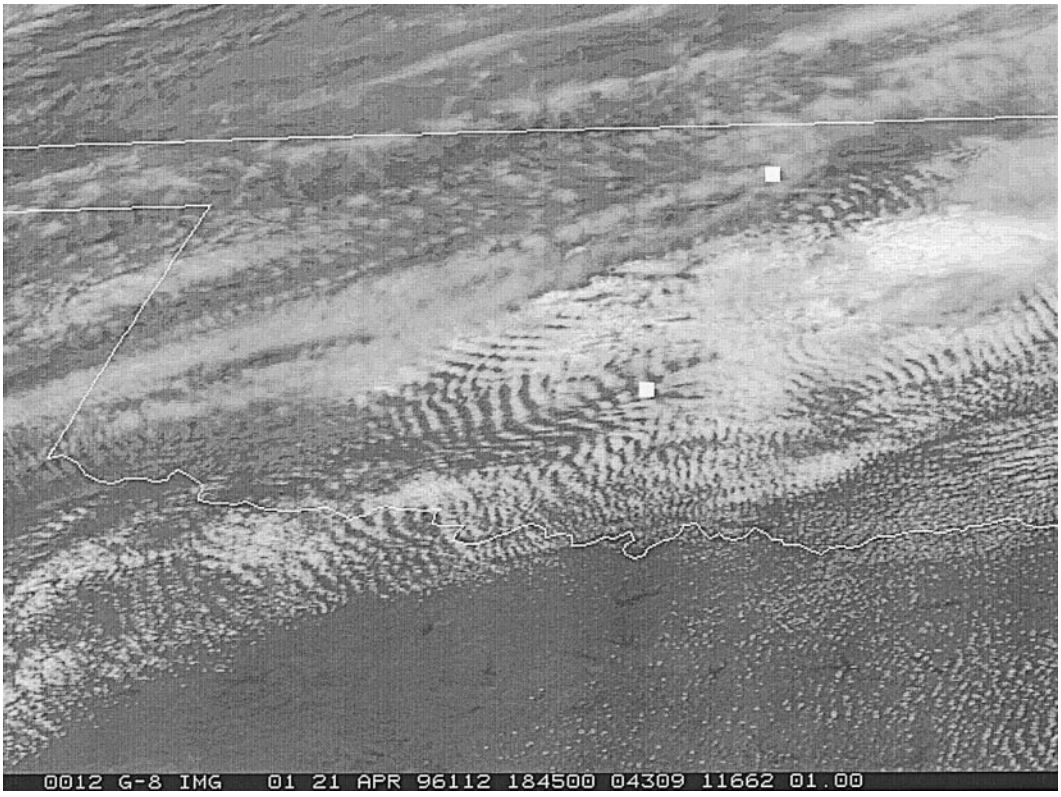


FIG. 2. The *GOES-8* (eastern) satellite image of Oklahoma at 1845 UTC. The white square marks the position of CART (north) and Purcell, Oklahoma (south).

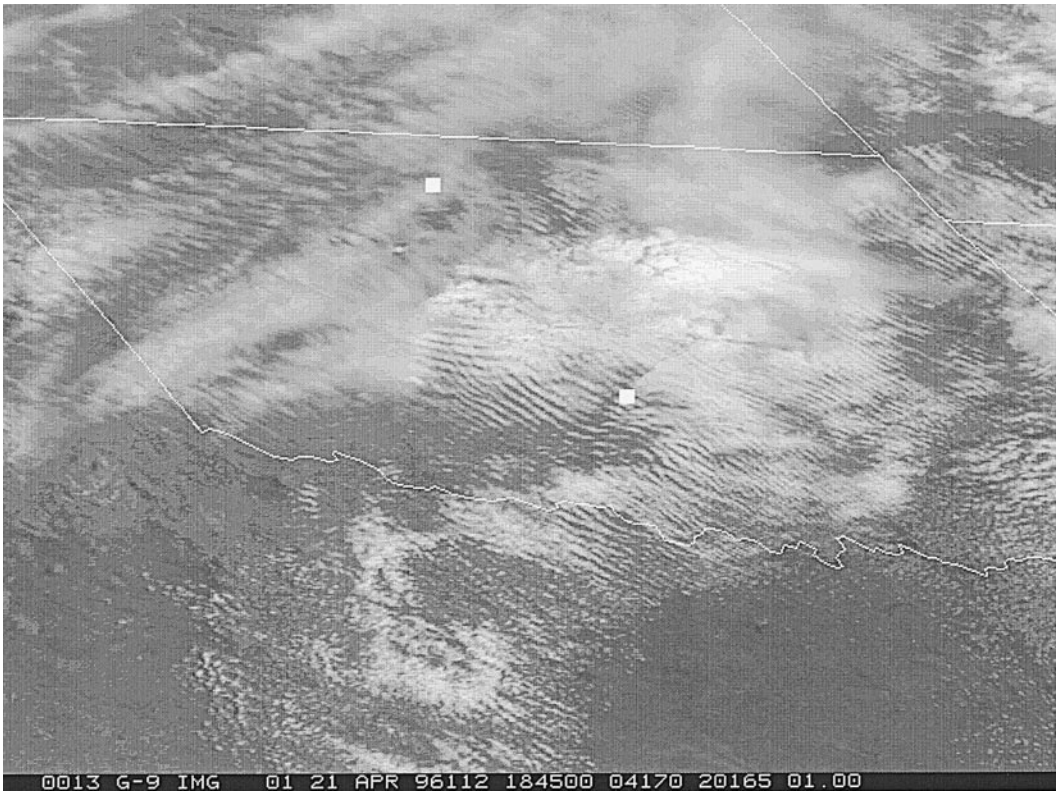


Fig. 3. The *GOES-9* (western) satellite image of Oklahoma at 1845 UTC. The white square marks the position of CART (north) and Purcell, Oklahoma (south).

the cloud's altitude and the satellite viewing angle from zenith.

Parallax shifts are not obvious to most users of satellite data because they use imagery from only one satellite view. However, when views from two different satellites are compared, the parallax shift becomes obvious.

To estimate the altitude of the cloud, we repeat the location calculation assuming the cloud is above the surface. This is illustrated in Fig. 1. The apparent parallax displacement on the earth's surface from two satellite views is indicated by distance $d_0$. A second displacement can be calculated by assuming the cloud is 1 km above the surface, $d_1$. Since the cloud depicted in Fig. 1 is above the 1-km altitude, we expect $d_1 < d_0$. We repeat this calculation every 0.5 km in the vertical. At the correct altitude of the cloud, the parallax displacement ($d_c$) approaches 0; that is, $d_c = 0$.

In the real world, two factors intervene to prevent $d_c$ from reaching 0: 1) the object used to define the cloud differs in appearance between the two satellite views and 2) the granularity of the satellite image.

To make a stereoscopic height measurement, a textural feature of the cloud needs to be precisely located in each satellite image. Examples of the satellite images are shown in Fig. 2 (*GOES-8,* the ''east'' satellite) and Fig. 3 (*GOES-9,* the ''west'' satellite). The appearance of the cloud pattern differs radically because of the different viewing geometry and the cloud's scattering of sunlight. *GOES-8* is closer to the cloud targets in Oklahoma (approximately 35°N, 97°W) than *GOES-9. GOES-8* is located at the equator and 75°W, while *GOES-9* is at the equator and 135°W. Therefore, clouds appear more elongated in the *GOES-9* image.

To find the same textural feature in both satellite images, the *GOES-9* image was remapped into the projection of the *GOES-8* image (see Fig. 4). This removes the distortion from the different viewing geometries. However, the remapped image appears to have less textural detail for some clouds.

The brightness of cloud objects depends on the scattering of sunlight in the cloud and the relative angles between the sun and the satellite. For this reason, the same textural features appear less vivid in one satellite image with respect to the other even after correction for viewing geometry. The sun was near local noon for the example shown here. The relative angle from the sun to the satellite was slightly smaller for *GOES-8* than *GOES-9.* Image differences from scattering geometry become larger away from local solar noon.

Cloud scattering of visible radiation to the satellite is complicated inside diffuse ice clouds. Wylie and Menzel (1989) concluded that the visible images of cirrus were not of the cloud top or cloud edge but were

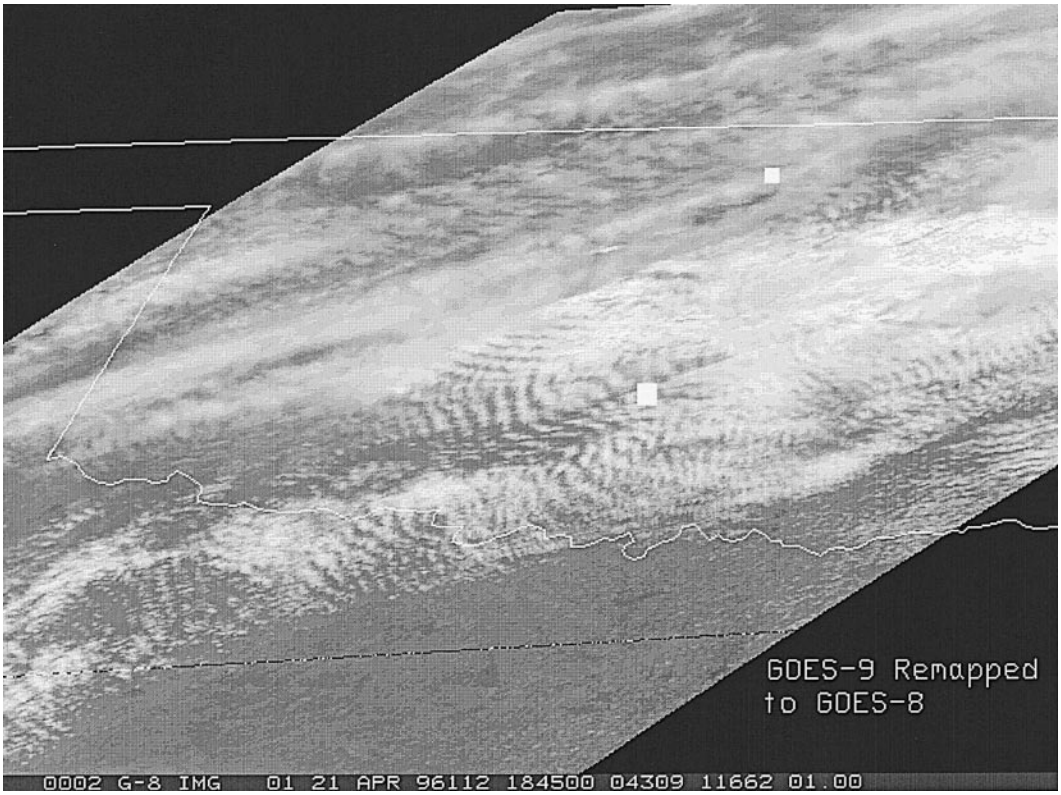


FIG. 4. *GOES-9* data remapped into the projection of the *GOES-8* image.

views into the interior of these diffusely reflecting clouds. They reached this conclusion after comparing cloud-top heights derived from the 13–15-$\mu$m $CO_2$ absorption with stereoscopic cloud height estimates. The heights derived from $CO_2$ absorption should have been lower than the cloud top because the absorption occurs inside the cloud (Wielicki and Coakley 1981). For a diffuse cloud, the level derived from $CO_2$ absorption should be closer to the middle of the cloud rather than cloud top. This was confirmed by Wylie and Menzel (1989) comparing the $CO_2$ cloud height estimates with lidar data. However, Wylie and Menzel (1989) also compared their $CO_2$ cloud heights to stereoscopic data and found little bias. This indicated that the stereoscopic technique also produced a low bias in cirrus cloud-top heights. Wylie and Menzel (1989) concluded that the stereoscopic views of the cirrus clouds tended to be of the scattering mass inside the cloud and not of the cloud-top surface.

Liao et al. (1996) examined Stratospheric Aerosol and Gas Experiment II (SAGE-II) data and found that many clouds have diffuse tops even if their lower layers are very dense. About one-half of the clouds detected in the SAGE-II data had these diffuse tops, implying that a definition of a cloud top is often difficult.

The second major error source for stereoscopic measurements is the granularity of the satellite images. *GOES-8* and *GOES-9* produce images of 1-km granularity at nadir. This granularity produced an error in the cloud's location since it was described in these data only to the nearest image pixel. Hasler et al. (1991) discuss the use of image correlation techniques to reduce the granularity somewhat below the size of a satellite pixel (1 km). However, image correlation is still hampered by the problems of radiative scattering differences between the satellite views.

The result of the errors in locating cloud textural features in the two satellite images is that the pointing vectors from each satellite shown in Fig. 1 do not actually intersect. Perfect intersection can only be achieved if the same textural feature can be accurately located in each satellite image and the radiative scattering of the cloud does not distort this feature between the two satellite views.

The important feature of our application of Hasler's (1981) technique is that $d_c$ is calculated for a variety of levels and not assumed to converge, $d_c \neq 0$. An example is shown in Table 1. The parallax displacement $d_c$ decreases with height to a minimum of 0.5 km at 11.5-km altitude. The azimuth angle also reverses direction at this altitude. This indicates that the pointing vectors from the two satellites come within to 0.5 km at 11.5 km above the earth's surface and then diverge. Thus, the best estimate of cloud height is 11.5 km at the location of 36.09°N, 96.42°W.

The error calculation gives an indication of the qual-

TABLE 1. An example of parallax errors ($d_c$) for one cloud target as a function of altitude. Altitudes are in kilometers, and latitudes and longitudes in decimal degrees. The azimuth is the angle of $d_c$ clockwise from north.

| | | | *GOES-8* | | *GOES-9* | |
|---|---|---|---|---|---|---|
| Altitude | Error | Azimuth | Latitude (N) | Longitude (W) | Latitude (N) | Longitude (W) |
| 0.0 | 22.2 | 89.1 | 36.190 | 96.495 | 36.193 | 96.247 |
| 0.5 | 21.3 | 89.1 | 36.186 | 96.492 | 36.188 | 96.255 |
| 1.0 | 20.3 | 89.1 | 36.181 | 96.488 | 36.184 | 96.262 |
| 1.5 | 19.4 | 89.1 | 36.177 | 96.485 | 36.180 | 96.269 |
| 2.0 | 18.4 | 89.2 | 36.173 | 96.482 | 36.175 | 96.276 |
| 2.5 | 17.5 | 89.2 | 36.169 | 96.478 | 36.171 | 96.284 |
| 3.0 | 16.5 | 89.3 | 36.165 | 96.475 | 36.167 | 96.291 |
| 3.5 | 15.6 | 89.3 | 36.161 | 96.472 | 36.162 | 96.298 |
| 4.0 | 14.6 | 89.3 | 36.157 | 96.468 | 36.158 | 96.305 |
| 4.5 | 13.7 | 89.4 | 36.153 | 96.465 | 36.154 | 96.313 |
| 5.0 | 12.7 | 89.5 | 36.148 | 96.462 | 36.149 | 96.320 |
| 5.5 | 11.8 | 89.6 | 36.144 | 96.458 | 36.145 | 96.327 |
| 6.0 | 10.8 | 89.7 | 36.140 | 96.455 | 36.141 | 96.334 |
| 6.5 | 9.9 | 89.9 | 36.136 | 96.452 | 36.136 | 96.342 |
| 7.0 | 8.9 | 89.9 | 36.132 | 96.448 | 36.132 | 96.349 |
| 7.5 | 8.0 | 90.1 | 36.128 | 96.445 | 36.128 | 96.356 |
| 8.0 | 7.0 | 90.3 | 36.124 | 96.442 | 36.123 | 96.363 |
| 8.5 | 6.1 | 90.5 | 36.120 | 96.438 | 36.119 | 96.370 |
| 9.0 | 5.1 | 90.9 | 36.116 | 96.435 | 36.115 | 96.378 |
| 9.5 | 4.2 | 91.5 | 36.111 | 96.432 | 36.111 | 96.385 |
| 10.0 | 3.3 | 92.3 | 36.107 | 96.428 | 36.106 | 96.392 |
| 10.5 | 2.3 | 93.8 | 36.103 | 96.425 | 36.102 | 96.399 |
| 11.0 | 1.4 | 97.4 | 36.099 | 96.422 | 36.098 | 96.406 |
| 11.5 | 0.5 | 180.0 | 36.095 | 96.418 | 36.093 | 96.414 |
| 12.0 | 0.6 | 180.0 | 36.091 | 96.415 | 36.089 | 96.421 |
| 12.5 | 1.5 | 260.5 | 36.087 | 96.412 | 36.085 | 96.428 |
| 13.0 | 2.4 | 263.6 | 36.083 | 96.408 | 36.080 | 96.435 |
| 13.5 | 3.4 | 265.0 | 36.079 | 96.405 | 36.076 | 96.442 |
| 14.0 | 4.3 | 265.8 | 36.075 | 96.402 | 36.072 | 96.450 |
| 14.5 | 5.3 | 266.3 | 36.071 | 96.398 | 36.067 | 96.457 |
| 15.0 | 6.2 | 266.7 | 36.066 | 96.395 | 36.063 | 96.464 |

ity of the cloud height estimate. Targets with large errors indicate a problem with the selected location in either or both of the images. All targets were selected manually in this example. When the error exceeded 0.9 km ($d_c > 0.9$), the target was rejected and another target was selected. We assumed that, where $d_c > 0.9$, a mistake was made in target selection or that the target, be it a bright spot or edge dark spot, was not seen in one of the images.

One problem with semitransparent cirrus is that the appearance of a bright spot can come from radiative scattering from more than one cloud layer. Lower layers often contribute to the brightness on an image. Thus, the apparent parallax displacement ($d_c$) may not represent the cirrus but rather correspond to that of a lower cloud feature. Hasler and Morris (1984) analyzed lower cumulus under a light cirrus canopy created by a hurricane, illustrating the complicated structure of clouds and their stereoscopic appearances.

Stereoscopic measurements also require perfect alignment of the satellite images. The registration does not have to be perfect by itself. But any shift between the two satellites will be mistaken for a parallax shift. Hasler (1981), Mack et al. (1984), and Wylie and Menzel (1989) all compared clear areas in each of the satellite images looking for registration shifts. In the old GOES system, some corrections had to be made based on the positions of lakes, rivers, and coastal outlines. One of the images was manually shifted to align with the other using the positions of landmarks. In the 1845 and 1915 UTC images of *GOES-8* and *GOES-9*, some small lakes in southern Oklahoma were visible. No apparent shift was seen in the locations of these lakes. Thus, manual registration corrections were not necessary for these data.

Stereoscopic measurements also require close coordination in the time of scanning the clouds. The motions of the clouds between the scans of the two satellites will cause errors in the height calculations. For the images used here, the time separation of the scans at 35°N, 97°W was only 13.0 s between the satellites. This information was extracted from the time record of the imager's scan. Correspondingly, a 40 m $s^{-1}$ cloud motion (the largest wind speed in the area) would produce only a 0.5-km height error. This cloud motion could only be mistaken for a cloud height if it were in the direction of the stereo parallax shift. In this case, the motion of the cirrus was within 20° of the stereo parallax. However, the close coordination in scan time of this area ensured that the largest error was less than 0.5 km.

It should be noted that not all GOES scans are so

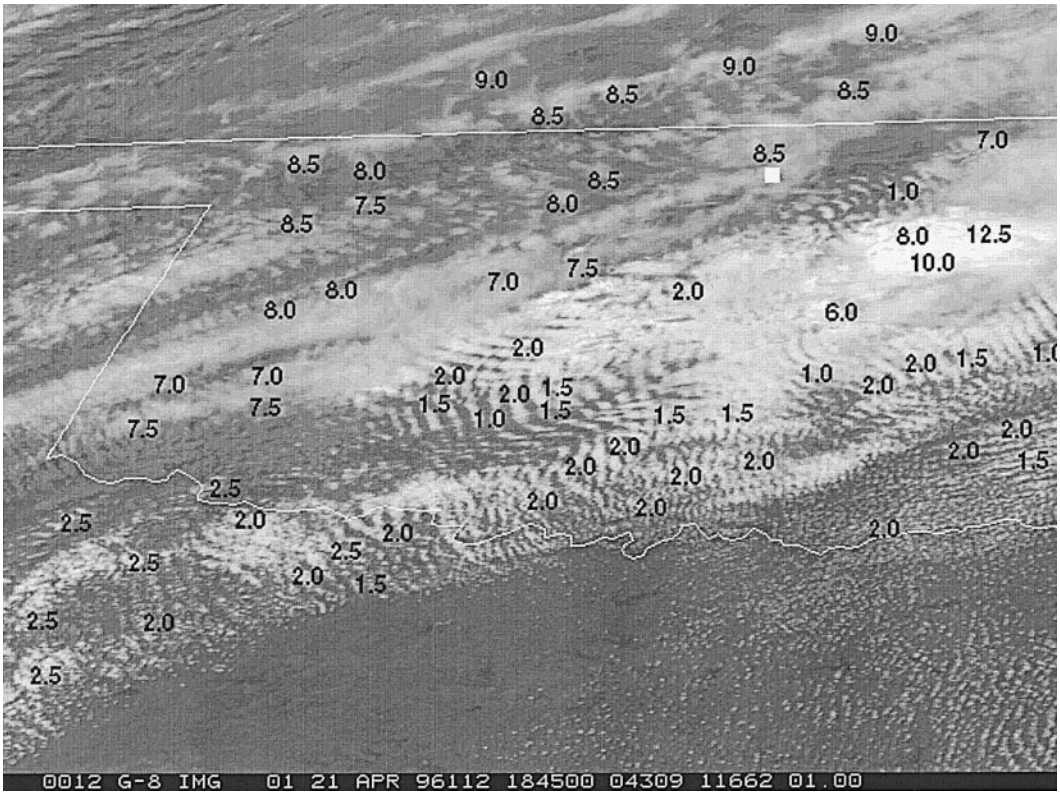


FIG. 5. Cloud heights (km) measured from the *GOES-8* and *-9* stereoscopic pair at 1845 UTC. The satellite image is from *GOES-8*.

closely coordinated in time. Another possible stereoscopic pair was scanned at a nominal time of 1745 UTC. However, the scan records indicate a 94.9-s difference at 35°N, 97°W. This would have produced possible height error of 3.8 km for a 40 m $s^{-1}$ cloud motion.

## 3. Case study

Two analyses of the stereoscopic cloud heights in Oklahoma on 21 April 1996 are shown in Figs. 5 and 6 at 1845 and 1915 UTC, respectively. The purpose of making stereoscopic measurements was to determine the height of the wave cloud patterns seen on the satellite images south and east of the Atmospheric Radiation Measurement (ARM) Program's Climate and Radiation Testbed (CART; ARM 1990; Stokes and Schwartz 1994). The ARM CART site near Ponca City, Oklahoma, is designated by the northern white square. SUCCESS flew several aircraft over the CART site along a southwest–northeast line and several sensors made simultaneous measurements from the ground at CART. Wavelike variations also were seen in many of the CART cirrus data, for example, Demoz et al. (1998). We needed to know if these were the same waves that appeared southeast of the cirrus on the satellite image.

A rawinsonde released at 1729 UTC at the CART site indicated high relative humidity in the boundary layer up to just above 1 km and then a dry layer to 6 km (see Fig. 7). Higher humidity also was found in the region from 6 to 10 km with some indication of layering. This midlevel moisture layering was even more evident in the sounding taken to the south at Purcell, Oklahoma (Fig. 7). The tropopause was located at about 13 km.

A highly sensitive downward-looking lidar on NASA's ER-2 aircraft indicated that the highest cirrus cloud tops were generally located at about the 11-km level (see http://virl.gsfc.nasa.gov). At times, several cloud layers were present in the 6–11-km layer, as indicated by observations from the ER-2 cloud lidar and from the Pennsylvania State University ground-based 95-GHz radar at the CART site (http://wwwarc.essc.psu.edu/datasets/nasasuccs.html). The radar observations indicate that the bulk of the cloud ice mass occurred in one or more layers located between 6 and 9 km and that the cirrus layer at 10–11 km was optically thin by comparison. Other quick-look data products can be found at the SUCCESS World Wide Web site (http://cloudl.arc.nasa.gov/success/index.html).

The satellite measurements clearly indicate that the wave clouds vividly seen on the satellite images were located in the boundary layer. Stereoscopic cloud heights of 0.5–2.5 km were calculated. Soundings at the CART site and to the south at Purcell, Oklahoma, both indicate that the depth of the moist boundary layer was

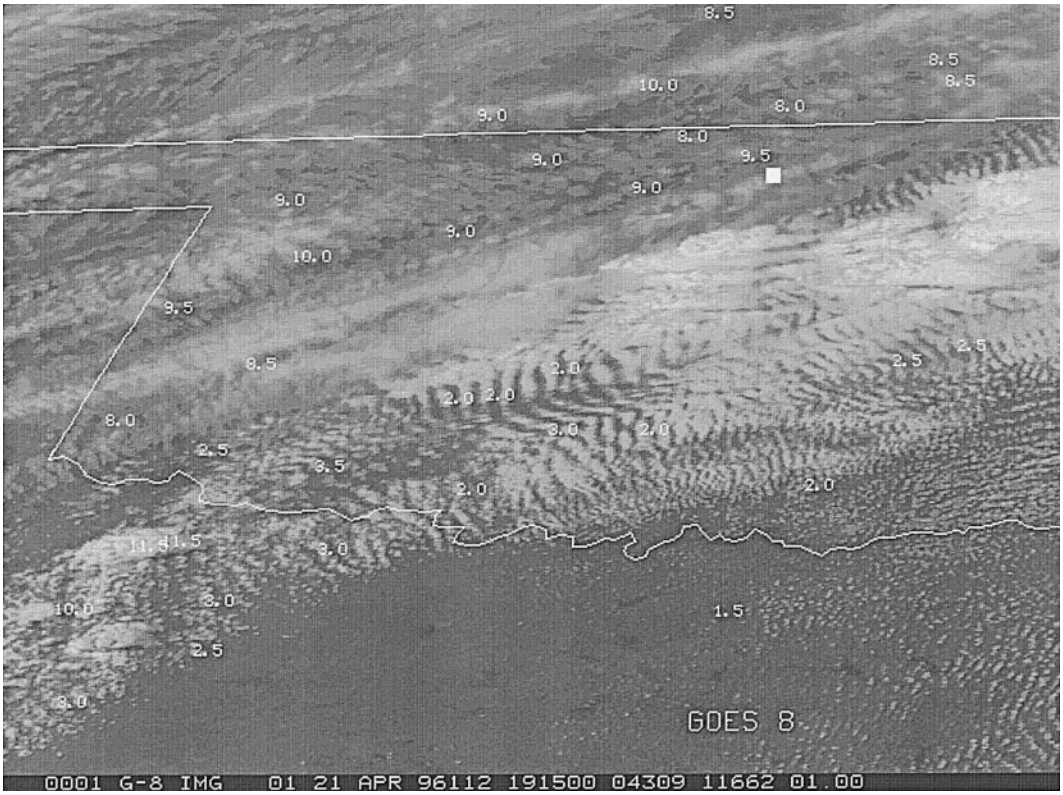


FIG. 6. Cloud heights from the 1915 UTC *GOES-8* and *-9* images.

confined to below 1.5 km, which is slightly lower than some of the stereoscopic estimates. The 11-$\mu$m blackbody temperatures, measured by *GOES-8* at a location far from the cirrus, were 285 K corresponding to a 1.8-km height (top of the inversion) on the CART and Purcell soundings. Nevertheless, these wave clouds were clearly below the 6-km level where the midlevel cirrus clouds were observed.

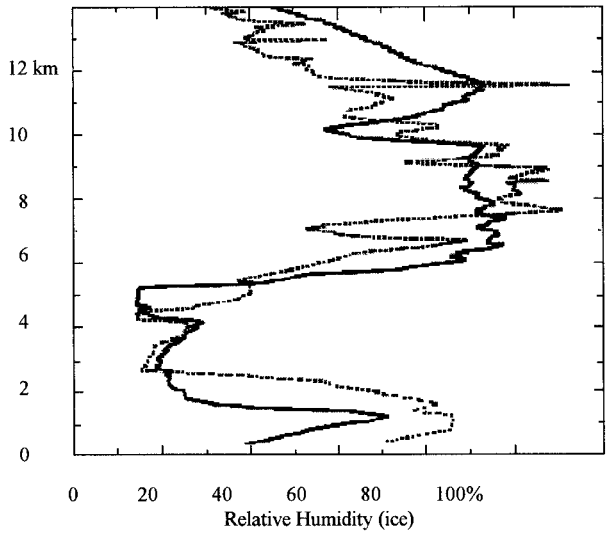


FIG. 7. The relative humidity with respect to ice from the soundings launched from the CART site (solid line) and Purcell, Oklahoma (dashed line). Locations of the sites can be seen in Fig. 2.

Cloud motions also indicated that the wave clouds that were located to the south of the CART site were in the boundary layer. The clouds moved north-northeast from 160° to 180° (Fig. 8). This agreed with the low-level winds observed both at the CART site and at Purcell (Fig. 9).

Stereoscopic heights of the cirrus located to the west of the CART site ranged from 7 to 9 km. These heights were less than the cloud-top heights derived from downward-looking lidar and are probably a result of the diffuse nature of these cirrus clouds, as discussed in the previous section. This is especially likely given the radar observations, which suggest that the brighter features used for the calculations likely occurred in the 6–9-km cloud layer.

A small cumulonimbus complex was evident to the southeast of the CART site (Fig. 5) where the stereoscopic cloud heights ranged from 8.0 to 12.5 km. Appropriate textural features were difficult to find on this cloud because of the large parallax displacement and the complex nature of the cloud top. The 12.5-km point came from tracking a brightness contour that appeared to be a downwind shadow of the anvil on a lower cloud. Cirrus also were present to the southwest of this Cb

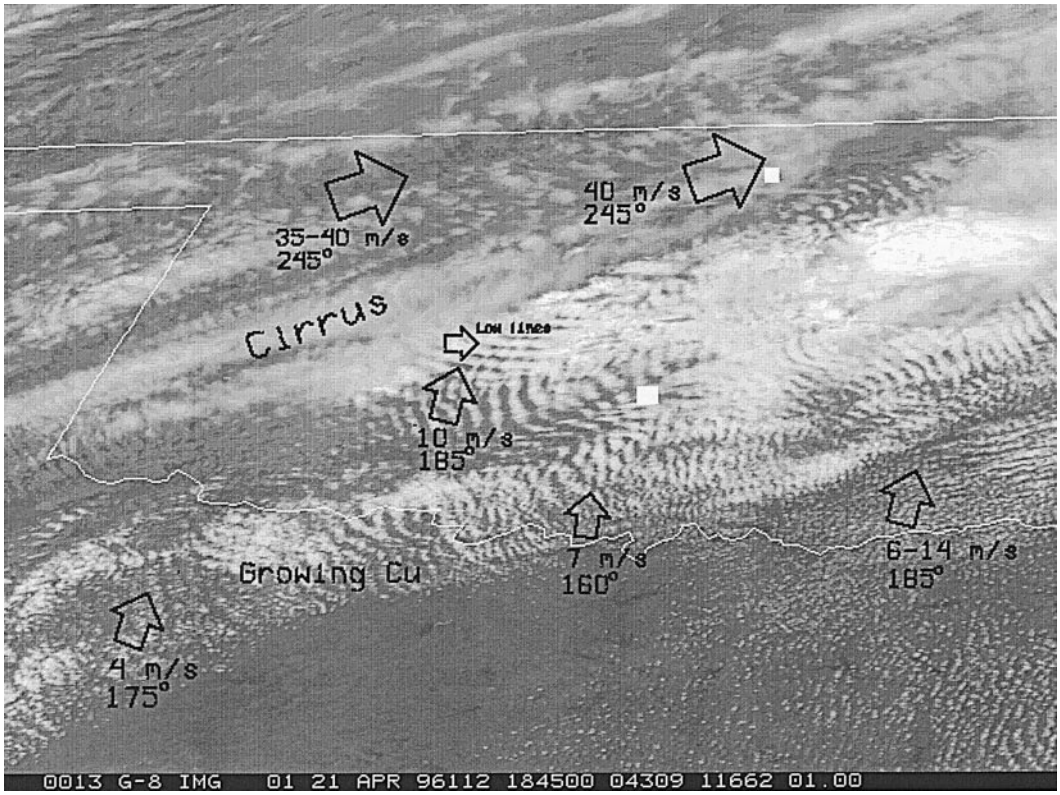


FIG. 8. The motions of the clouds (m $s^{-1}$) (directions are azimuth the clouds come from).

complex. However, textural patterns were difficult to analyze there.

## 4. Summary and conclusions

The stereoscopic measurements indicated that the wave clouds vividly seen on the satellite images south and east of CART were not part of the cirrus that moved over CART from the west. Cloud motions, satellite-measured blackbody radiances, and radiosonde humidity profiles all indicate that these wave clouds were boundary layer clouds. There is some disagreement as to their top heights. Stereoscopic measurements indicate tops up to 2.5 km, while radiosonde humidity profiles indicate strong drying above 1.8 km. This difference, 0.7 km, is about the expected error of stereoscopic measurements from the previous discussion and prior analysis of Hasler (1981).

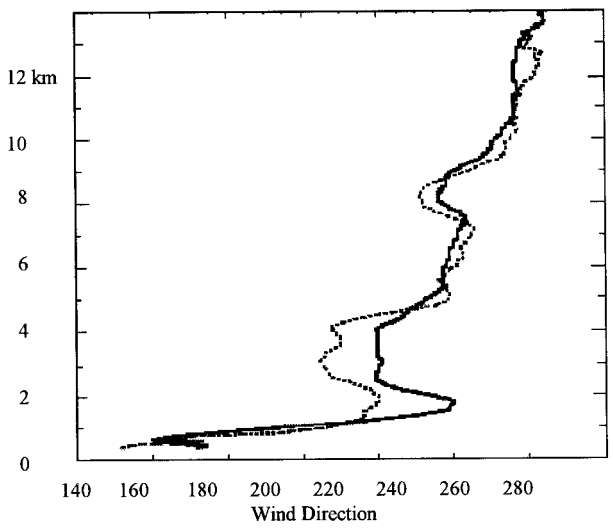


FIG. 9. The wind directions from the soundings at CART (solid line) and Purcell, Oklahoma (dashed line).

The stereoscopic heights of the cirrus over and west of CART appear to be below the highest cloud tops recorded by the ER-2 lidar and also well below the tropopause. Radiosonde data and other CART data indicate possible cloud layers from 6 to 11 km. The stereoscopic data appear near the middle of this range, 7–9 km. This follows the conclusion reached by Wylie and Menzel (1989) using the older GOES data, that stereoscopic cloud height measurements of diffuse cirrus are biased low, below the true cloud top. This bias occurs because the image seen by the satellite is of scattering within the cloud and not from its top surface. In this case, the scattering is likely dominated by the denser cirrus layers located from 6 to 9 km. The lidar also is more sensitive to the small concentrations of cloud particles near the cloud's top, which may be invisible on the GOES images. Using this small dataset, the height bias appears to be

about 2 km, similar to that reported in Wylie and Menzel (1989).

The largest surprise of this study is the quality of the *GOES-8* and *-9* data. Registration corrections were normally made on all data used from the old GOES system. The lack of need for these corrections here came as a surprise. However, other GOES users have indicated that the registration quality varies through out the day (T. Schmit 1997, personal communication). The best registration appears to come during daylight, while large errors have been found at night. This is a different behavior than the previous GOES system. The previous GOES registration errors tended to be constant through out the 24-h day. Registration errors could be predicted for several hours using empirical measurements. The new GOES system does not have this predictability, and registration errors need to be checked on every stereoscopic pair.

The time coordination of the two satellites also came as a surprise. The previous GOES system had large differences in time sampling that were partially caused by limited data-handling resources on the ground. Coordinated images for stereoscopic data were collected only for very short periods. The *GOES-8* and *-9* data used here were not intentionally scheduled for stereoscopic measurements. The authors retrieved the data from the archive and asked if such measurements were possible. The success of these measurements implies that stereoscopic cloud height data could possibly be extracted on a routine basis from operational data, as proposed by Hasler et al. (1991).

The clarity of *GOES-8* and *-9* images over the previous satellites is also better, which aids in locating cloud textural features. The dynamic range of digitization of the visible image uses a 10-bit scale, which is an improvement over the 6-bit scale used in the past. Also, the visible images are oversampled in the scanning process (approximately the east–west direction of each scan) by a factor of 1.7. This also enhanced the image clarity.

As a final note, the application of satellite stereoscopic cloud height measurements is not limited to only the U.S. GOES satellites. As proposed by Hasler et al. (1991), stereoscopic data could be collected with NOAA Advanced Very High Resolution Radiometer and GOES for limited regions. This possibility should be considered.

*Acknowledgments.* This work was supported by NASA Grants NAG1-1830 and NAG1-553. The authors also thank the reviewers for providing very helpful and positive comments, which greatly improved this manuscript.

## REFERENCES

ARM, 1990: Atmospheric Radiation Measurement Program Plan Executive Summary. U.S. Department of Energy, DOE/ER-0442, 19 pp.

Demoz, B. B., D. O'C. Starr, S. Bowen, and R. Chan, 1998: Wavelet analysis of dynamical processes in cirrus clouds. *Geophys. Res. Lett.,* in press.

Fujita, T. T., 1982: Principle of stereoscopic height computations and their applications to stratospheric cirrus over severe thunderstorms. *J. Meteor. Soc. Japan,* **60,** 355–368.

Hasler, A. F., 1981: Stereoscopic observations from satellites: An important new tool for the atmospheric sciences. *Bull. Amer. Meteor. Soc.,* **62,** 194–212.

——, and K. R. Morris, 1984: Stereoscopic satellite observations of hurricanes: An update. Preprints, *15th Tech. Conf. Hurricanes and Tropical Meteorology,* Miami, FL, Amer. Meteor. Soc., 132–139.

——, R. Mack,, and A. Negri, 1983: Stereoscopic observations from meteorological satellites. *Adv. Space Res.,* **2,** 105–113.

——, J. Strong, R. H. Woodward, and H. Pierce, 1991: Automatic analysis of stereoscopic satellite image pairs for determination of cloud-top height and structure. *J. Appl. Meteor.,* **30,** 257–281.

Liao, X., W. B. Rossow, and D. Rind, 1996: Comparison between SAGE II and ISCCP high-level clouds 2. Locating cloud tops. *J. Geophys. Res.,* **100,** 1137–1165.

Mack, R., A. F. Hasler, and R. F. Adler, 1983: Thunderstorm cloud top observations using satellite stereoscopy. *Mon. Wea. Rev.,* **111,** 1949–1964.

Rodgers, E., R. Mack, and A. F. Hasler, 1983: A satellite stereoscopic technique to estimate tropical cyclone intensity. *Mon. Wea. Rev.,* **111,** 1599–1610.

Menzel, W. P., and J. F. W. Purdom, 1994: Introducing GOES-I: The first of a new generation of geostationary operational environmental satellites. *Bull. Amer. Meteor. Soc.,* **75,** 757–781.

——, D. P. Wylie, and K. I. Strabala, 1992: Seasonal and diurnal changes in cirrus clouds as seen in four years of observations with the VAS. *J. Appl. Meteor.,* **31,** 370–385.

Minnis, P., K. N. Liou, and Y. Takano, 1993a: Inference of cirrus cloud properties using satellite-observed visible and infrared radiances. Part I: Parameterization of radiance. *J. Atmos. Sci.,* **50,** 1279–1304.

——, P. W. Heck, and D. F. Young, 1993b: Inference of cirrus cloud properties using satellite-observed visible and infrared radiances. Part II: Verification of theoretical cirrus radiative properties. *J. Atmos. Sci.,* **50,** 1305–1322.

Platt, C. M. R., and G. L. Stephens, 1980: The interpretation of remotely sensed high cloud emittances. *J. Atmos. Sci.,* **37,** 2314–2322.

Rossow, W. B., 1989: Measuring cloud properties from space: A review. *J. Climate,* **2,** 201–213.

——, and R. A. Schiffer, 1991: ISCCP cloud data products. *Bull. Amer. Meteor. Soc.,* **72,** 2–20.

——, and L. C. Gardner, 1993: Cloud detection using satellite measurements of infrared and visible radiances for ISCCP. *J. Climate,* **6,** 2341–2369.

Stokes, G. M., and S. E. Schwartz, 1994: The Atmospheric Radiation Measurement (ARM) Program: Programmatic background and design of the cloud and radiation test bed. *Bull. Amer. Meteor. Soc.,* **75,** 1201–1221.

Susskind, J., D. Retuter, and M. T. Chaine, 1987: Cloud fields retrieved from HIRS/MSU data. *J. Geophys. Res.,* **92**(D), 4035–4050.

Wielicki, B. A., and J. A. Coakley, 1981: Cloud retrieval using infrared sounder data: Error analysis. *J. Appl. Meteor.,* **20,** 157–169.

——, and B. Parker, 1992: On the determination of cloud cover from satellite sensors: The effects of sensor spatial resolutions. *J. Geophys. Res.,* **97,** 12 799–12 823.

Wylie, D. P., and W. P. Menzel, 1989: Two years of cloud cover statistics using VAS. *J. Climate,* **2,** 380–392.

——, ——, H. M. Woolf, and K. I. Strabala, 1994: Four years of global cirrus cloud statistics using HIRS. *J. Climate,* **7,** 1972–1986.